Computational design, fabrication and evaluation of rubber protein models

Thomas Alderighi[a,b,*], Daniela Giorgi[a], Luigi Malomo[a], Paolo Cignoni[a], Monica Zoppè[c,d,*]

[a]*ISTI - CNR, Italy*
[b]*Università di Pisa, Italy*
[c]*IBF - CNR, Italy*
[d]*Dipartimento di Bioscienze, Università di Milano, Italy*

ARTICLE INFO

ABSTRACT

Tangible 3D molecular models conceptualize complex phenomena in a stimulating and engaging format. This is especially true for learning environments, where additive manufacturing is increasingly used to produce teaching aids for chemical education. However, the 3D models presented previously are limited in the type of molecules they can represent and the amount of information they carry. In addition, they have little role in representing complex biological entities such as proteins. We present the first complete workflow for the fabrication of soft models of complex proteins of any size. We leverage on molding technologies to generate accurate, soft models which incorporate both spatial and functional aspects of large molecules. Our method covers the whole pipeline from molecular surface preparation and editing to actual 3D model fabrication. The models fabricated with our strategy can be used as aids to illustrate biological functional behavior, such as assembly in quaternary structure and docking mechanisms, which are difficult to convey with traditional visualization methods. We applied the proposed framework to fabricate a set of 3D protein models, and we validated the appeal of our approach in a classroom setting.

1. Introduction

Physical models of atomic assemblies and small molecular structures provide a human-scale representation of entities that are too small to be perceived directly. The tangible nature of physical reproductions triggers different cognitive and perceptual processes than exclusively visual stimuli alone, and it enables the perception and manipulation of spatial relationships and mechanisms. Therefore, tangible 3D molecular models can conceptualize complex phenomena in a stimulating and engaging format, which well complements computer-generated graphical representations. This is especially true for learning environments, such as undergraduate schools, where tangible models of molecular structures can help teachers to illustrate concepts in chemistry and biology.

The widespread diffusion and low cost of 3D printing has been accompanied by the increasing interest in and application of additive manufacturing for chemical education. The recent surveys [1, 2, 3, 4] and the references therein show how 3D printed teaching aids are increasingly entering chemistry

---

*Co-corresponding authors:
   e-mail:* thomas.alderighi@isti.cnr.it (Thomas Alderighi), monica.zoppe@cnr.it (Monica Zoppè)
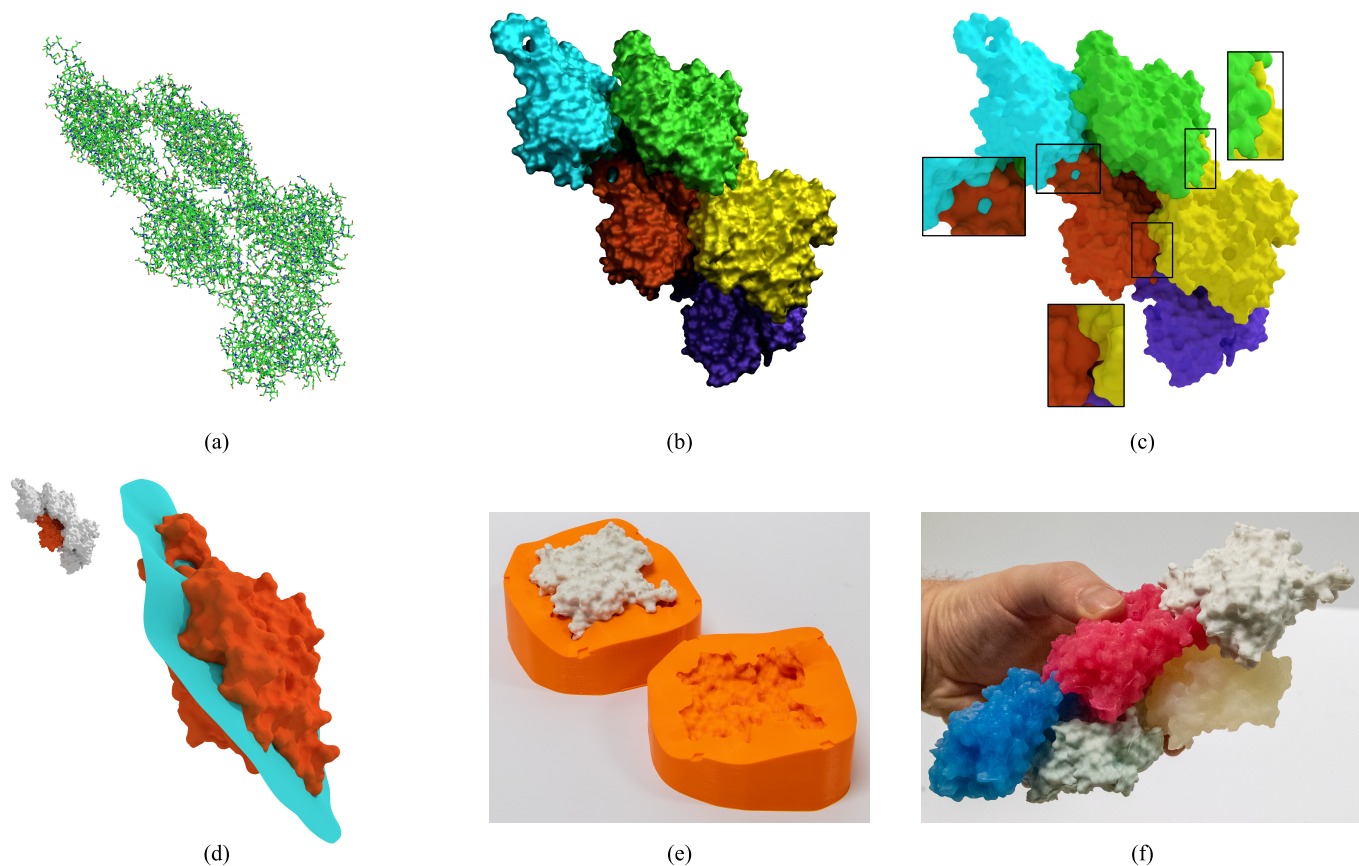
Fig. 1. An overview o f the proposed pipeline, demonstrated on F-actin. Top, surface generation: atom representation of the PDB record file (a); extracting the monomers solvent excluded surfaces (b); interpolating exactly matching surfaces (c). Bottom, 3D fabrication: determining the mold parting surface (d); 3D printing the mold and casting the monomer (e); multiple cast of the monomers are assembled to form a fraction of the F-actin filament (f).

classrooms. Models and kits with 3D printed representations of molecular structures have been used in chemistry pedagogy to teach, for example, orbital theory and molecular symmetry [5, 6], and a positive correlation was found between the introduction of 3D printed teaching aids and student learning [7, 8].

Nevertheless, the majority of 3D models presented so far are limited in the type of molecules they can represent, up to tens of atoms, and the amount of information they carry. They are best suited for general and organic chemistry, while they only play a small role in representing biological entities such as proteins, which are typically composed of thousands of atoms organized in complex 3D geometry. Moreover, proteins are *flexible* entities, often working in dynamic groups, and are capable of deforming upon interaction with each other to form quaternary structures or ligand-receptor complexes. Nevertheless, most existing physical models of molecular surfaces are *rigid* (see, for example, [9, 10, 11]) and it can be difficult, especially for

students, to grasp the flexible and 'adaptive' nature of protein-protein interactions.

We present the first complete workflow for the fabrication of *soft* models of complex proteins of any size. We leverage on molding and casting technologies to generate accurate models which can incorporate both spatial and functional aspects of large molecules such as proteins.

Our workflow covers the whole pipeline from molecular surface preparation and editing (Figure 1a,b,c) to actual 3D model fabrication (Figure 1d,e,f). The surface generation part includes the editing of contact surfaces in interaction sites, and topological checks to tell apart biologically-meaningful features from reconstruction noise. The fabrication part includes the automatic design of mold pieces for casting rubber protein models with complex geometries; and a strategy to visually and numerically inspect molding results prior to fabrication to prevent and eventually fix unsuccessful molds.

Our fabrication technique is time- and cost-effective. It enables the manufacturing of multiple copies of accurate and functional physical models of large protein complexes, currently not feasible with state-of-the-art techniques. Models fabricated with our strategy can be used as aids to illustrate biological functional behavior, such as assembly in quaternary structure and docking mechanisms, which are difficult to convey with traditional methods. A better understanding of the way proteins work facilitates teaching at high and superior grade courses, and will possibly inspire biologically-based reasoning in both scholars and lay persons.

We present a set of fabricated models, namely monomers of F-actin, the alpha and beta monomers of hemoglobin, and fused dimers (H2A/H2B and H3/H4) to compose the histone octamer. The models are freely available and downloadable from the NIH database [12] and can be used by anyone willing to print the molds and cast the proteins in soft material, in schools or other settings.

The coronavirus emergency prevented us from performing a large user study to validate the effectiveness of our models in either labs or formal teaching environments. Nevertheless, we gave our models to two science teachers of two high schools in Italy, who managed to use them in their classes after the partial re-opening of high schools in January 2021. We collected their feedback, overall very positive, and report here their experience and suggestions.

The article layout is as follows. In Section 2 we briefly revise the state of the art about tangible models in biology and chemistry. Section 3 introduces the steps in our pipeline, which are then detailed in Section 4 (surface generation and editing) and Section 5 (mold design and fabrication process) respectively. Section 6 presents our fabricated models, and Section 7 their evaluation in a classroom setting. Discussions and conclusions in Section 8 end the article.

2. State of the art

The opportunity of building and using physical models for a better understanding of proteins and their components was recognized since the early days with the seminal work from Corey and Pauling [13]. With time, several attempts have been made using disparate materials and techniques: notably, the Myoglobin model by Kendrew et al. [14], reproducing the folding of the main chain, and the more sophisticated all atoms models, again by Kendrew in 1969, now at the Science Museum in London. These models were built by scientists for their use, to help them understand the properties of proteins, the behavior of the main chain and side chain atoms, and also for displaying the results of their studies to colleagues and other scholars. These models, however, were very cumbersome to build and to handle, and much of the protein studies and reporting have relied on indirect information. Today, in most cases, students' first encounter with proteins is through their sequence, activity, location, molecular weight, post-translational modifications and more. Protein interactions are typically referred to the primary sequence, rather than to their 3D surface. Molecular structures are often displayed as 2D images in textbooks, and printed relative to the size of the paper, so that it is extremely difficult for unexperienced viewers to perceive the absolute and relative size of the objects.

The advent of interactive computer graphics has enabled the representation of biological objects in some details starting from the '80s of last century, and today there are many packages capable of producing powerful CG representations on the basis of the atomic coordinates [15, 16]. However, the theoretical usefulness of physical models has always been recognized, as demonstrated by the many studies reporting attempts to provide such models.

One of the barriers to the wide adoption of tangible models as teaching aids has been their cost, which could be prohibitive for the majority of teaching environments. The advent of desktop 3D printers has partially addressed this issue: the estimated cost of 3D printed molecular structures designed with freeware CAD software is one fiftieth of the price of commercially available models [6]. Affordable 3D printing of molecular models has been encouraged in recent years supported by the creation of free web repositories like the NIH 3D Print Exchange [12], and is gaining some traction, as testified by the website users.

Herman et al. [9] prepared several models, either by 3D printing or using flexible wires covered with foam, to demonstrate the folding process, i.e. emphasizing the main chain secondary structure, and demonstrated their use in biochemistry classes in high schools. Art Olson demonstrated the self-assembly of icosahedral viral capsid using 3D printed units mimicking polyovirus coat protein complexes, equipped with small magnets [17].

However, the process of printing is time-consuming, and, more importantly, hard plastic is unsuited for demonstrating many relevant features of proteins, such as their flexibility, and often cannot be used for building multi-subunit complexes. Kawakami [18] proposed the production of models that integrate information about both the internal structure, represented by a ribbon or wire frame 'skeleton', and the surface, made with transparent rubber. The models are used to assemble multi-subunits complexes, with the aid of magnets, and allow exploration of the quaternary structures. However, the strategy of the construction method is not explained, and, as far as we know, the process has not been replicated.

In summary, physical models are widely used in the field of general and organic chemistry, and their role is widely recognized as tools to build mental images, permitting the elaboration of complex chemical structures [3]. However, for large molecules like proteins, their use has been limited to few cases, also due to their cost and difficult production.

Here we report the pipeline for relatively easy and cheap reproduction of multiple copies of protein models, all at the same scale, that can be adopted in many setting.

3. Overview

Our aim is to define a pipeline for fabricating physical 3D protein models of any complexity. We target models of proteins able to demonstrate the association of subunits. We want the models to be soft, so that their manipulation demonstrates the importance of a degree of flexibility to allow associations. We also target geometrically-complex models, to demonstrate the relevance of *disordered domains* in nature.

The input to our algorithm is a macromolecular structure represented in a PDB (Protein Data Bank [19]) record file, which lists the 3D coordinates of all atoms in the protein (Figure 1a). We use PyMOL [20] to extract the mesh representing the solvent excluded molecular surface (SES [21]). In the case of multimers, each monomer is extracted as a single surface mesh (Figure 1b). Since we are interested in modeling the interaction between adjacent monomers, we want the surfaces to be exactly matching in correspondence of the interaction sites. Indeed, having matching surfaces makes it easier to detect the interaction areas and to match the two monomers. However, extracting the surfaces independently for each monomer often leads to difficult to match surfaces, or even to intersecting surfaces, which makes it impossible to reach a correct match. To solve this, we automatically identify the contact areas between the monomers, and we locally interpolate a common surface between the monomers (Figure 1c), as detailed in Section 4.1.

Finally, we adjust the surface topology, so that it matches the biological properties of the molecule. Protein folding often produces structures in which parts that are distant in the primary sequence are brought to proximity, giving rise to loops that may be more or less stable, depending on many forces intrinsic of the proteins (hydrophobic interactions and H-bonds) and on external conditions (like pH, temperature, presence of ions and/or ligands etc.). In geometrical terms, these loops correspond to topological handles that may or may not correspond to biologically meaningful molecular features. Sometimes, handles can also arise due to artifacts of the SES extraction process. We propose a strategy to automatically remove topological handles corresponding to noise, after they are told apart from chemically-justified ones by visual inspection of the model, detailed in Section 4.2.

Once obtained the interpolated and topologically-simplified surfaces of monomers, we proceed to define the fabrication step. Our aim is to fabricate soft models of molecules with complex geometries, in multiple copies. Therefore, we opted for *casting* as a fabrication strategy, rather than 3D printing. Casting techniques require the design of a mold with an empty

cavity shaped like the target object. The cavity is filled with a liquid casting material such as resin or silicone. Once the material has cured, the mold is opened to extract the reproduced object. Casting techniques ensure high geometric accuracy, and better scale with the number of copies than 3D printing, since a single mold can be reused to fabricate multiple objects. Furthermore, casting techniques support a wide spectrum of materials, including rubber, whereas, as of today, it is not possible to print soft silicone materials using commercial 3D printing technologies. However, the geometric complexity of shapes that are fabricable by casting is more limited in comparison to 3D printing, and significant effort has to be invested to design moldable shapes and the mold itself [22, 23].

The main problem to be faced when designing a mold is deciding how the mold should open up and detach from the cast object during extraction. In other words, one needs to decide what are the *parting surfaces* that will cut through the mold volume, separating it into multiple parts, and what are the *parting directions* along which the mold pieces will open.

When targeting the generation of rigid molds, the choice of the optimal parting directions and surfaces should account for the presence of *undercuts*, namely parts of a mold piece that face an opposite direction with respect to its extraction direction, since undercuts will render the mold ineffective. The inset shows a synthetic description of how undercuts can occur and affect the mold: the mold surface is depicted in orange, while the object is represented in turquoise; the red-striped parts are undercuts and the object would get stuck there during a rigid extraction procedure.
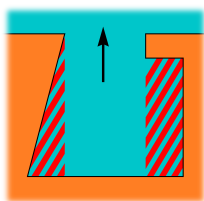
In our case, the use of a soft material to cast the molecule inside our molds allows us to relax some constraints that characterize the generation of rigid molds. Indeed, the flexibility of the material would cope with mild undercuts. Nevertheless, organic shapes, such as biological complexes, feature intricate geometrical details, so that the design of valid parting surfaces still remains a hard problem.

Previous works mainly addressed *soft molding* for *rigid* objects [24, 25]. Instead, we target *rigid molding* for *soft* objects. The extension of existing solutions is not straightforward. Therefore, we build on [24, 25] to define a new strategy for rigid casting of soft objects, customized for the reproduction of molecular structures, as explained in Section 5. We first define parting directions and surfaces that minimize the presence of undercuts (Figure 1d). Then, we define two heuristics to evaluate the feasibility of the rigid molding process. In case of predicted failure, the user can opt for the use of soft molds, instead of rigid ones. Though, the casting process would become much more complex: it would require an additional casting for the mold, beside the casting of the object. Moreover, if both the mold and the object are made of soft material, the detaching process can become tricky due to the potential binding between the mold and the object when using affine materials for the two. Therefore, we propose a visualization of the molding result to allow the user to decide on the best casting strategy, namely, rigid mold/soft object (Figure 1e) versus soft mold/soft object.

The final step, after the fabrication of monomers, is the assembly of the multi-subunit complex (Figure 1f).

4. Molecular surface preparation

The first step of our workflow is the extraction of the molecular surface (SES) of the desired macromolecule from the PDB file of atomic 3D coordinates (Figure 2 left).

We rely on the PyMOL API to fetch a molecule from the PDB repository and inspect it before continuing the pipeline. At this stage, a user can select the relevant chains to be modelled, deciding whether to include or exclude accessory molecules (such as water, oligosaccharide chains, prostethic groups or accessory proteins). Given the selected subunits, we extract the SES using the implementation provided in PyMOL (Figure 2 right). In all our experiments, we used a probe radius of 1.4Å.

The set of subunit surfaces is the input to the subsequent geometry processing pipeline, to locally edit the surfaces and prepare them for fabrication.
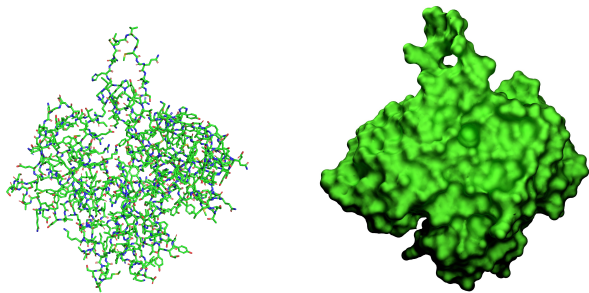
Fig. 2. The all atoms representation of the F-actin monomer and the corresponding solvent excluded surface. This surface will be the input geometry of our method.

4.1. Local surface editing at interacting areas

Solvent excluded surfaces, by construction, do not allow for a solid and intuitive match between interacting areas. In fact, when extracting the surface of each subunit independently, intersecting surfaces and high-frequency geometric details make it impossible to match interacting areas.

To enforce a correct match between surfaces along the interacting areas, we propose an interpolation scheme to locally alter the subunit surfaces, providing perfectly matching and smooth surfaces in correspondence of contact areas. Figure 3 top shows a detail of one of the interaction sites between two F-actin monomers before and after the surface interpolation procedure.

Our interpolation scheme works on an implicit representation of the subunits surfaces. Given a subunit A and its surface, the input of the interpolation scheme is a pair of distance fields: the distance field D_A holding the signed distance from A's solvent excluded surface; and the distance field D_{other} holding the signed distance to the surfaces of the other subunits composing the protein assembly. Conceptually, we are looking for a field $\overline{D}_A$, such that its $0-$isosurface will approximate to a medial surface (with respect to its interacting subunit surfaces) locally to interacting areas, and smoothly converge to the original surface moving away from the interaction. We define a threshold distance t ($t = 1.4$Å, the water molecular radius) and locally interpolate the fields where the two subunits are closer than t (see the sketch in Figure 3 bottom). If the two subunits are closer than t, we want the 0-isosurface of $\overline{D}_A$ to approximate the medial surface between the two t-isosurfaces (red line in Figure 3

bottom right). Otherwise the $0-$isosurface of $\overline{D}_A$ should match the original surface (black line). The transition between the medial and the original surfaces should be as smooth as possible (fading blue line).

To achieve this, we define $\overline{D}_A$ as:

$$\overline{D}_A = \begin{cases} D_A & \text{if } D_A \geq t \text{ or } D_A \cdot D_{other} \leq 0 \\ D_A - D_{other} & \text{if } D_{other} \leq t \\ (1 - \lambda)\,(D_A - t) + \lambda\,D_A & \text{otherwise} \end{cases}$$
(1)

where

$$\lambda = \frac{2}{(1 + e^{-kr})} - 1, \quad r = D_{other} - t$$

is a sigmoid function that smoothly converges to 0 when D_{other} goes to t and smoothly converges to 1 as D_{other} grows. The parameter k of the sigmoid controls the steepness of the curve: lower values will result in wider areas of interest for the interacting site interpolation, while higher values will result in a faster convergence to the original surface.

We apply the interpolation scheme to every subunit in the protein assembly, to obtain perfectly-matching surfaces for later fabrication and assembly. The interpolation process locally modifies the SES surface, to an extent that can be controlled by tuning parameters t (offset radius) and k (sigmoid shape) in Eq. 1. In our experiments, we used an offset radius $t = 1.4$Å (the water molecular radius) and $k = 0.65$.

The approximation produces a surface that is closer to the interaction surface than to the monomer SES. However, it is well known that proteins are dynamic entities, that polymeric forms might be more static than free subunits, and that crystallized forms represent only a single snapshot, possibly not even the most representative of the cellular population. Therefore, the approximation is acceptable to illustrate associations in molecular complexes.

4.2. Topological simplification

When targeting the surface of macromolecular ternary structures, topological handles that do not correspond to chemically
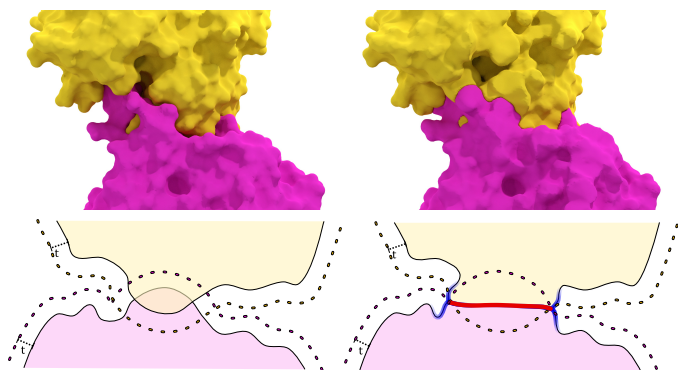
Fig. 3. The solvent excluded surface (top left) can present intersections and geometric details that would make the matching between interacting subunits difficult (bottom left). Our local surface editing method ensures that two interacting subunits will perfectly match in the interaction region, while preserving the original surface away from those regions (right).

linked surfaces can arise as artifacts due to the SES extraction process (Figure 4). These handles should be removed to reflect the correct connectivity pattern of atoms.

First, we automatically locate surface handles following the method by Dey et al. [26]. Then, for each handle that should be removed, we compute a minimal handle loop (roughly speaking, the shortest loop that bounds the molecular surface interior across the handle; Figure 5 left). We generate the approximate minimal surface enclosed by the loop using Poisson reconstruction [27], then generate an offset surface of this minimal surface. Finally, we subtract the offset surface from the original model via CSG boolean operation [28] (Figure 5 right). The effect of this operation is to break any noisy handle loop on the molecule surface, reducing the surface topological complexity until it matches its biological nature.

The handle removal process is automatic, apart from the identification of biologically relevant handles which is left to the human expert.

4.3. Alignment

In cases of complexes comprising several subunits, one can use the same mold for fabricating identical subunits, if their reconstructed surfaces are perfecty aligned. Though, in many cases the crystal structure of each identical subunit is not exactly identical: while the sequence of aminoacids is the same and the main chain atoms are nearly overlapping, the side chains, especially in surface residues, are often found in slightly
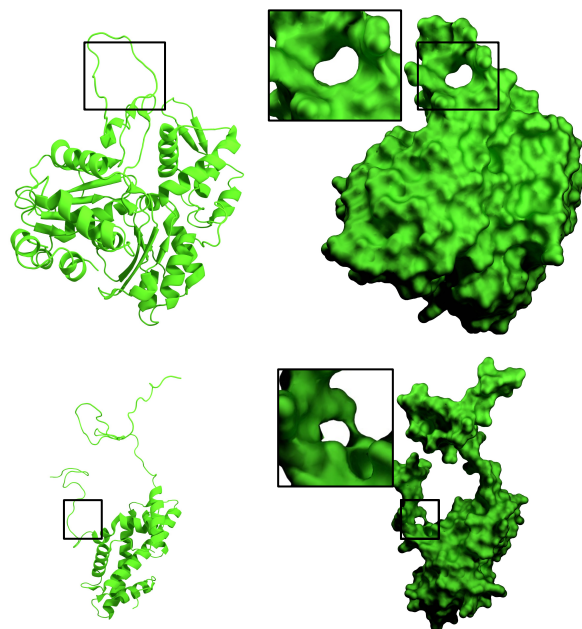

Fig. 4. In the case of the F-actin monomer the protein structure itself features a topological handle (top), while the topological handle on the SES from the histone dimer is an artifact of the SES extraction process (bottom).
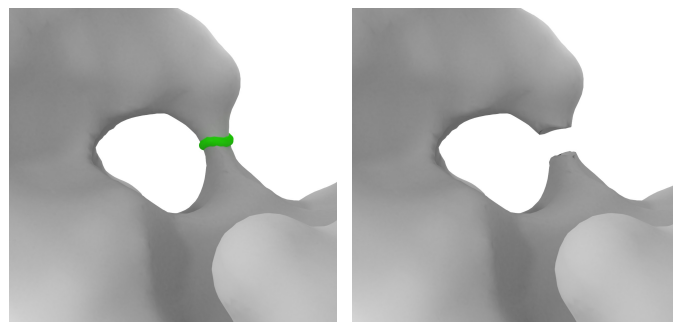

Fig. 5. A minimal handle loop, highlighted in green (left); the local editing of the surface to break the handle (right).

different configurations. This is biologically expected, as thermal vibration, the presence of water and ions in the solvent and random fluctuations, all contribute to the dynamic motion of the proteins surfaces. To align the identical subunits surfaces, we used Coot [29] and ccp4 [30], and built perfectly overlapping subunits to be used for subsequent elaborations.

5. Mold generation

Once the subunits surfaces have been computed, we can proceed to design the geometry of the corresponding molds required for their fabrication.

5.1. Computation of parting surfaces

To design a two-piece mold, the first step is to identify the two parting directions and the corresponding parting surface. The parting directions are the directions along which to extract the mold pieces; the parting surface is the surface decomposing the target object into two parts, each one assigned to a mold piece.

We start with the method illustrated by Alderighi et al. [25], which was designed for soft molds and rigid cast objects. First, we choose as parting directions the pair of directions that minimize the undercut area of the subunit surface. We uniformly sample a set of candidate parting directions on the unit sphere. For each candidate direction, we use GPU-accelerated rendering to compute the visible and non-visible surface areas, as proxies for undercuts. Then, we select as parting directions the two directions which minimize the non-visible surface area. As in [25] we use these parting directions to determine a decomposition of the mold interior volume in two mold pieces. The parting surface is given by the boundary separating the two volume parts (Figure 6 left). See [25] for additional details.

The parting surfaces define the geometry of the two-piece rigid mold (Figure 6 right), which we fabricate via 3D printing. The method described in [25] exposes a parameter ϵ in the parting surface generation algorithm, which controls the shape of parting surface. We empirically experimented different values of ϵ and found $\epsilon = 0.1$ to give good results, as discussed in Section 6.

The assumption behind minimizing undercut areas is that mild undercuts are tolerated when using flexible casting materials, such as rubber. This is true in the general case, therefore our method is able to produce valid rigid molds for a variety of complex molecular structures. This was the case with the F-actin and hemoglobin models in Figures 9 and 10. Although, macromolecules can feature a very complex and challenging geometry, as with the case of histones in Figure 11. In [25], which targeted soft, silicone molds for rigid objects, geometrical complexity was handled with additional cuts in the soft mold, that would allow its opening. This is not feasible in our setting, with
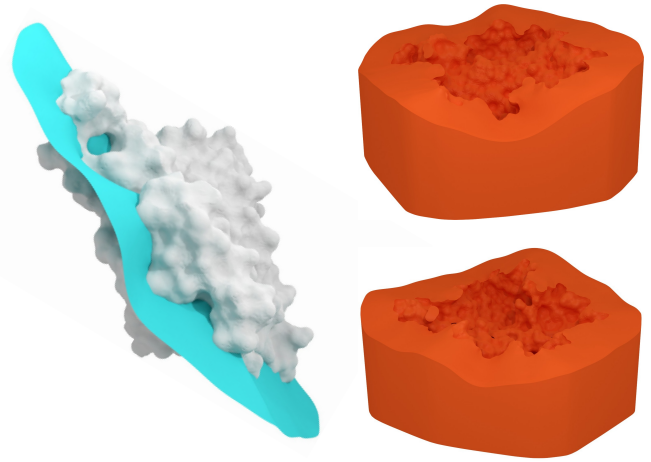

Fig. 6. On the left, the surface of the F-actin monomer (gray) cut by the parting surface (light blue). The parting surface defines the geometry of the mold pieces, on the right. The mold pieces are 3D printed.

a rigid mold and a soft object to cast. Therefore, it is not always possible to automatically generate a valid rigid two-piece mold. We opted to limit the design process to the generation of two-piece molds to simplify the fabrication and casting process. Indeed, more complex multi-piece rigids molds would allow to design valid rigid molds even for more complex protein structures but at the cost of a highly more complex casting process, with respect to soft-soft two piece molds.

In the next section, to overcome this limitation, we define two heuristics to forecast whether the rigid casting would be successful or not. In case of likely failure, one can opt for a fallback strategy relying on the use of soft molds for soft objects. Soft molding would be more complicated in terms of fabrication effort than rigid molding, therefore, rigid molding should be the first choice.

5.2. Evaluation of feasibility of rigid casting

In order to aid the detection of failure cases where our method would not be able to produce a valid rigid mold, we provide some heuristics that can, in a conservative way, warn the user about the unfeasibility of the rigid solution and suggest the use of the fallback soft mold generation algorithm.

In particular we define two heuristics: a stronger one, based on the topological analysis of the generated parting surface, and a softer one, based on the analysis of the undercuts introduced by the mold segmentation, giving an estimate of how difficult it

would be to safely extract the molecule from the mold itself.

Topological Check. This heuristic gives the user a strong necessary indication of whether the generated mold will be extractable or not. This topological check evaluates the topology of the mold parting surface. Assuming, without loss of generality, that the subunit molecular surface is made up of a single connected component, we consider the mold decomposition valid if and only if the parting surface has the topology of a disk with one hole (Figure 7 left). Whenever this condition is not satisfied this means that probably some part of the object is completely enclosed by one piece of the two-piece rigid mold, and portions of the object volume should be able to slide through it during the extraction process, see Figure 7 for a representation of the phenomenon.
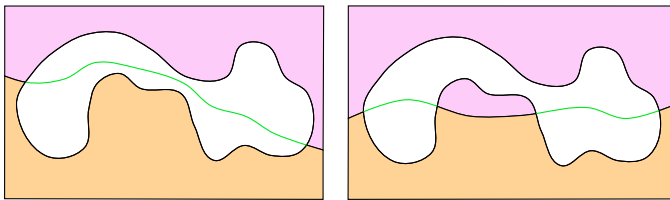

Fig. 7. A 2D diagram showing a mold decomposition where the parting surface is topologically equivalent to a disk with a single hole (left) or to a disk with two holes (right). In the latter case, it will be difficult or even impossible to extract the mold. The object is the white area; the upper and bottom mold pieces are pink and orange, respectively; and the green line stands for the hole(s) boundary (one on the left, two on the right).

Undercuts Estimation. This heuristic relies on a geometrical analysis of the undercuts introduced by the mold decomposition. We estimate the impact of undercuts using a geodesic-based measure. The measure accounts for how hard it would be to extract some part of an object surface that lies in undercut with respect to a given direction, according to the undercut *depth*. We estimate the depth of an undercut as the maximum geodesic distance of its points from the visible region according to the extraction direction. Figure 8 depicts this measure mapped to the surface color on the two mold pieces.

The depth for a model is the maximum depth of its undercuts. Indeed, the heuristic should warn the user about the possible unfeasibility of the mold decomposition, and even a failure extracting a single portion of the surface would render the whole

mold and reproduction invalid. In our experiments, we empirically found that decompositions that pass the topological check described above and whose undercut depth is below 9 mm are easily moldable using a rigid mold (see the results in Section 6), without the risk of damaging parts of the soft protein during extraction, due to the presence of undercuts.
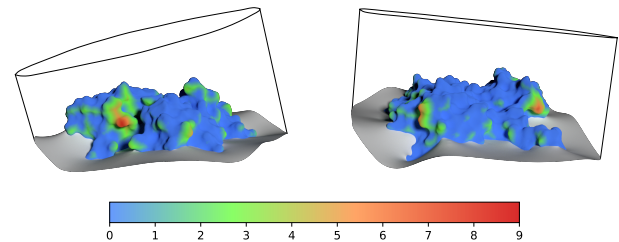

Fig. 8. A representation of the two rigid mold pieces for the F-actin monomer. The surface corresponding to the molecule surface has been painted according to the undercut depth measure (millimeters), defined as the geodesic distance from a point in undercut and the closest visible points.

For cases where using a rigid mold would result in an unfeasible mold, a fallback approach is to generate a soft, composite mold as in [25]. Thanks to the flexibility of a soft mold, the fallback strategy allows for the definition of additional cuts in the mold volume that can open and deform during the extraction procedure. This makes it possible to generate valid molds for a wide range of shapes, with complex topology and geometry, including surfaces representing complex molecular subunits. This comes with the cost of a more complicated fabrication process, since it needs the 3D printing of a rigid mold to cast the soft mold, and an additional casting step to produce the soft mold parts (see Figure 11).

5.3. Topological constraints

Finally, a hard constraint for rigid molding is posed by the presence of topological handles in the geometry to be cast. In presence of a topological handle it would be impossible to generate a valid rigid mold for a given macromolecule: the soft material would get stuck in a loop on the rigid mold making the extraction impossible without damaging the molecule [24]. To solve this issue, we use the topological simplification strategy defined in Section 4.2 for noisy handles, to break any handle loop on the molecule surface, reducing its topological complex-

ity until it is topologically equivalent to a sphere. From a fabrication point of view this will avoid the presence of handles in the rigid mold, and so ensure that the soft material can be extracted from the mold. Once the molecule is cast, the original topology can be restored by easily glueing together the handle using a fast curing silicone minimally altering the soft molecule appearance. Note that any topological handle that is cut through by the parting surface is implicitly opened by the cut surface itself, therefore the topological simplification process can be postponed until after the generation of the parting surface. This is the case for the actin monomer, as can be seen in Figure 6 left.

When targeting the soft-soft fabrication pipeline, the handle opening procedure can be avoided entirely since internal cuts in the flexible mold allow for the correct extraction of the object even in presence of handle loops.

5.4. Failure cases

Either the rigid-soft or the soft-soft strategies are expected to produce valid results for a wide range of complex structures. Both strategies are at risk of failure with bottle-shaped objects with very large cavities and small escape holes, as those would cause part of the mold to get stuck into the object cavity. At any rate, these features are not very common to molecular structures, to the best of our knowledge. These limitations are mostly intrinsic to the fabrication of objects using casting, rather than the mold design strategy itself. Finally, the soft nature of the objects also mitigates this problem.

6. Results

Among the many possible proteins, we have selected some of general interest and also appropriate to demonstrate the value of rubber fabrication: F-actin, the hemoglobin tetramer, and the histone octamer.

The number and variety of structures deposited in the Protein and Cryo-EM database is very large and constantly increasing. Selection of the proteins to fabricate was based on the possibility of demonstrating the association of subunits, identical or different, the importance of a degree of flexibility to allow such

association, and the relevance of complex geometrical structures. We excluded proteins whose structure is incomplete.

Finally, scale is an important consideration when fabricating molecular models. We decided for a size of the tangible molecular models equal to 10 millions times the size of the actual molecular structure [31]. This scale produced tangible models that can be easily held and manipulated. At the same time, keeping a fixed scale for all models proves beneficial for model comparison, avoiding confusion about relative dimensions.

The fabricated models are described and shown below, along with their molds.

F-actin. This model was chosen to demonstrate the possibility of polymerization. Starting from PDB model 6ANU, obtained by cryo-EM [32], the central monomer (chain A in the PDB file) was selected as a model, because it makes contact with four other monomers. Only a single rigid mold was necessary to fabricate many identical monomers. The rubber model can be analyzed as a monomer to reveal the interaction surfaces, and can be combined with more subunits to build a fragment of filament, like the assembly shown in Figure 9. The STL files for the F-Actin mold are downloadable at `https://3dprint.nih.gov/discover/3DPX-015176`

Fig. 9. The rigid 3D printed mold for the F-actin monomer and a fragment of filament assembled using five identical subunits cast from the same mold. To better appreciate the helical structure of the filament see Figure1.f.

Hemoglobin. This is a classic textbook example of tetrameric protein, composed of two alpha and two beta chains. The starting model used is PDB file 1GZX, of oxygenated hemoglobin obtained by X-ray crystallography [33]. For each of the two monomers the structures were aligned and adjusted in order to obtain identical structures, as described in Section 4.3. The heme component, including the iron atom and the oxygen molecule, were included in the molecular surface. Two independent molds were used for casting copies of alpha and beta monomers (Figure 10). The STL files for the hemoglobin alpha and beta chains are downloadable at `https://3dprint.nih. gov/discover/3DPX-015177`.
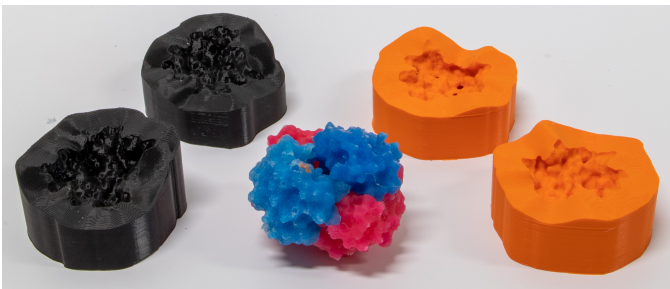

Fig. 10. The 3D printed rigid molds for the alpha (orange mold, blue cast) and beta (black mold, red cast) chains of the hemoglobin. In the center, the alpha and beta chains assembled to form the hemoglobin.

Histone octamer. This is the fundamental unit for DNA organization into Nucleosomes. We produced two pairs of dimers: H2A/H2B and H3/H4 (Figure 11). The model 1KX5 was obtained through X-ray crystallography [34] and includes also 147 base pairs of DNA. Because the model is produced at the 10 million $\times$ scale, DNA wrapping around the octamer can be simulated using a rope of 1 cm diameter, doubled and twisted to the appropriate degree (3.4 cm for a complete twist), like in Figure 12. The geometrical complexity of histones, with the N-terminal tails protruding from the core of the nucleosome and associating with DNA was considered a good example to demonstrate the relevance of disordered domains. Indeed, once assembled, it is very clear how the histone tails emerge from the nucleosome core, and are available for interaction with the many nuclear proteins involved in epigenetic marking of chromatin, and other nuclear processes.

Histone is an example of the proteins that cannot be cast directly with a rigid mold, using our technique. The geometric complexity of the molecular structure made it necessary to use the fallback strategy for the generation of a soft silicone mold. Using a silicone mold gives us more flexibility in terms of the attainable shapes, but results in a more cumbersome casting process (Figure 11). The STL files for the two dimers are available at `https://3dprint.nih.gov/discover/3DPX-015178`.
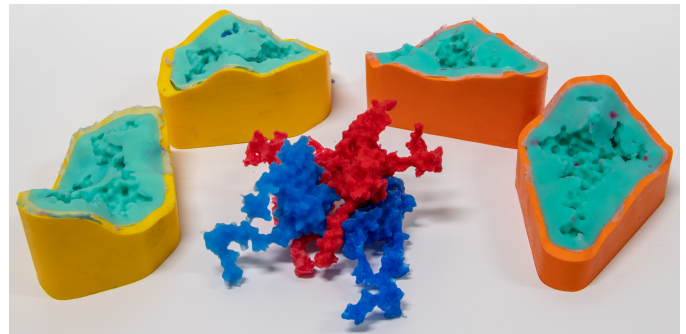

Fig. 11. The composite silicone molds for the creation of the histone dimers. The soft molds (turquoise) are cast using 3D printed metamolds.
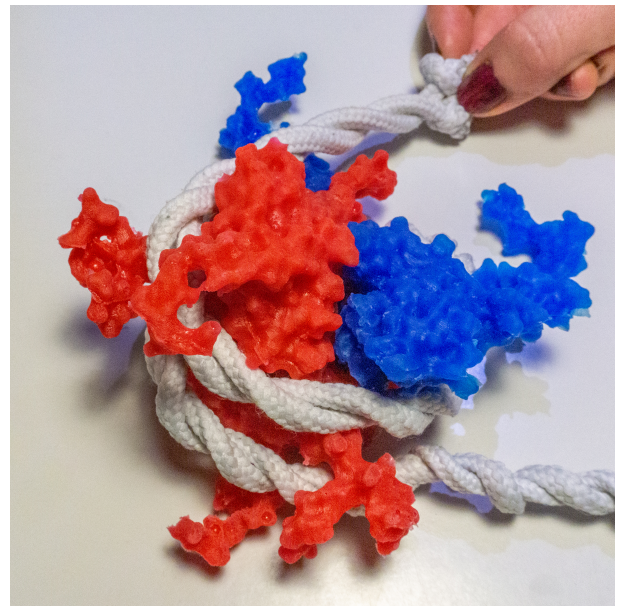

Fig. 12. DNA wrapping around the histone octamer. The DNA strand can be roughly simulated using a doubled and twisted rope.

Figure 13 shows the evaluation of the heuristics defined in Section 5.2 for the F-actin monomer (top) and the H2A-H2B histone dimer (bottom), according to different parameter values to generate the parting surfaces. Green bars mean that the out-

put passes the topological check, red bars mean failure to do so, while the y-values are the undercut depth estimation as described above. The figures show how the F-actin monomer can be cast using a rigid 3D printed mold, while the histone dimer requires a soft mold.
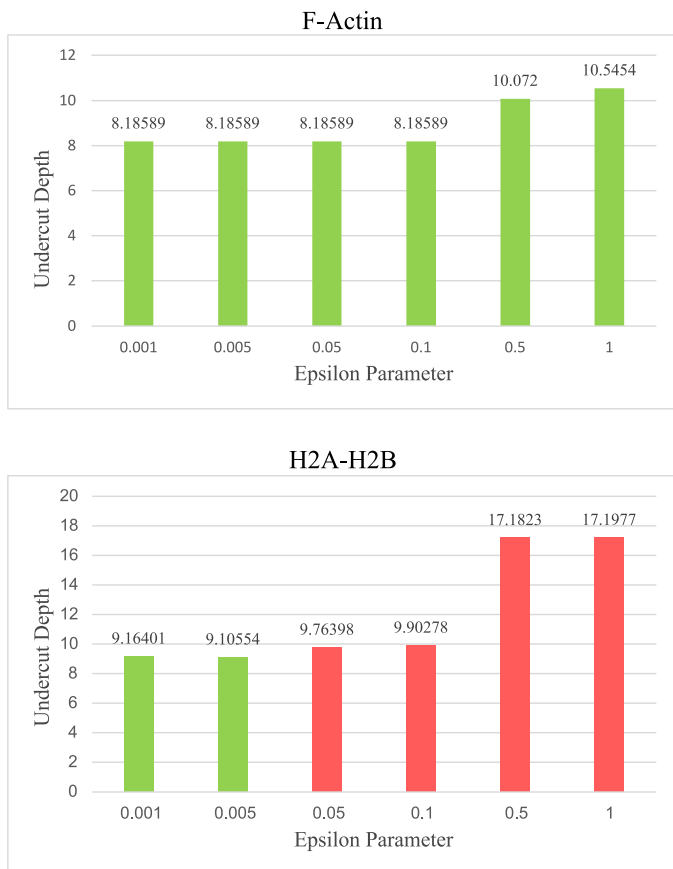

Fig. 13. Checks prior to mold fabrication for different values of the ϵ parameter controlling the geometry of the parting surfaces (see Section 5). Bar color depicts the outcome of the topological check: green is success, red is failure. The $y-$values are the undercut depth (in mm).

6.1. Expert in the loop

Our pipeline is semi-automatic, in that it requires an expert in the loop to decide on questions of biological relevance. Human input is required in the following steps:

Protein Selection The PDB repository is highly redundant, and so the user needs to carefully select the most appropriate PDB file for the desired protein.

Alignment of identical monomers (optional) Because proteins are active molecules, the precise location of their atoms is not fixed, even in the highly artificial conditions of a crystal. As a result, different subunits of identical atomic composition may show slightly different geometric conformations. Therefore, the exact reproduction of the protein complex would require fabricating an individual mold for each subunit. To limit the number of molds, one can resort to a manual alignment of subunits, followed by selection of a single set of atomic coordinates, a step that is best performed by expert crystallographers, using dedicated tools [29, 30], as discussed in Section 4.3. For the Hemoglobin and Histone models in this Section, this step required about an hour from an expert crystallographer. Note that the alignment step is optional; indeed, the choice between performing the alignment step and preparing more than one mold is up to the user.

Handle Removal/Preservation (optional) An expert has to decide on which are the topological handles to remove or preserve in the fabricated protein, according to their biological significance. This step is optional as it is not needed for the fabrication to be successful, since handles are automatically dealt with as described in Section 4.2. However, if significant handles are not preserved, the fidelity of the resulting model could be jeopardized.

Output Inspection As discussed in Section 5.2, our technique does not always succeed in generating a rigid mold for complex protein structures. However, the user can choose to switch to the fallback soft mold design strategy by looking at the *topological check* and *undercut estimation* results.

6.2. Implementation details

We used the PyMOL API and GUI to implement the operations required for fetching the PDB data, allowing the user to visually inspect the molecular data and eventually perform some molecular alignment operations if needed. SES surfaces are extracted using the PyMOL implementation of Connolly Surfaces [35]. We implemented the distance field transformation described in Section 4.1 using the OpenVDB library [36]. Finally the mold generation algorithm is implemented using the
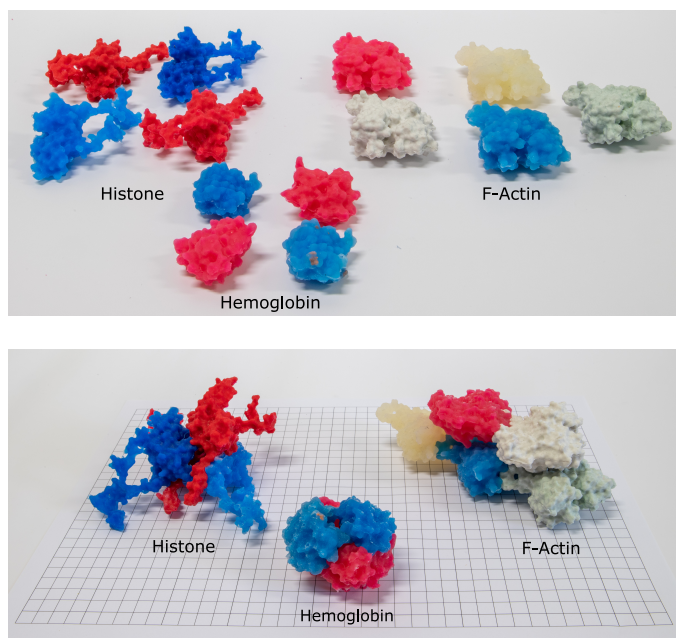
Fig. 14. Top: the protein subunits we provided as a teaching test kit to the high school teachers involved in the user evaluation. Bottom: the assembled proteins, on a centimeter grid for scale reference.

VCGLib [37]. The whole pipeline can be executed through an interactive Jupyter Notebook.

All the soft models and molds in the paper were created using common silicone rubbers with varying stiffness properties, with shore values ranging from 15A to 20A. All the different rubbers we tested are available at any hardware store. Cure times vary from 30 minutes to several hours depending on which silicone rubber is used. All the casting tests were conducted by inexperienced users (the authors, a computer scientist and a biologist). Once a mold is ready, each cast operation requires around 30 minutes of active work plus cure time.

7. Evaluation

Our tangible models can be employed in a number of situations, both in teaching and in research. In the last months, due to the coronavirus emergency, access to labs was restricted, and high schools were closed for most of the time in Italy. Even when schools re-opened, the sharing of material among students was forbidden. This prevented us from developing a larger and more complete user study. Nevertheless, we managed to test our models in a classroom setting, after high schools partially re-opened in January 2021.

7.1. Evaluation setup

We provided a set of models to two science teachers in two high schools, in different cities (Pisa and Milan). The teachers were not involved in the present work, and none of them knew our method prior to the evaluation test. The participation was on a voluntary basis, with no monetary reward.

Each teacher was provided with a full set (Figure 14 top) comprising: five monomers of F-actin, the four monomers of hemoglobin (two alpha and two beta), and four fused dimers (two H2A/H2B and two H3/H4) to compose the histone octamer. For training, composition of the complexes was demonstrated for F-actin in a short virtual live session with one of the authors, and for the other proteins with short videos of the assembly. Figure 14 bottom shows the assembled kit.

The teachers used the models as teaching aids during one of their lessons, as permitted by law due to COVID-19 restrictions: they brought the models in their classes, but students were not allowed to directly manipulate and share them. However, the students witnessed the teachers assemble the complexes, and could get a direct impression of their shape, complexity and size.

The types of high schools, the age and background of students, and the content of the lessons were different. This helped us to evaluate the usefulness of our models in different contexts. Teacher 1 used the models in two classes in 4th Liceo Scientifico (Science High School, age 17), in lessons about blood circulation: hemoglobin as an oxygen and CO_2 carrier, and actin as component of cardiac myocytes. The students were already familiar with the basic principles of cellular biology and of protein synthesis. Teacher 2 brought the models in a class of 2nd year in a technical school (mostly mechanical and electric preparatory, age 15), in a lesson about cells and proteins. In this case, the students had no previous classes of chemistry or biochemistry, and this lesson was their first encounter with proteins.

About the choice of the three proteins as test models, unfortunately the teachers were unable to demonstrate the histone octamers, because DNA organization was not in their programs

during the test period.

A few days after the lessons, both teachers reported their impressions in a short interview. They answered a set of specific questions, and also reported freely about their classroom experience. The interviews were not anonymous.

The evaluation is necessarily limited, given the contingent circumstances. At any rate, the feedback was very positive and encouraging, as detailed in the next section. A broader user study is planned for the future, as soon as the emergency situation allows it.

7.2. Evaluation results

The questions and summary of answers are reported in Table 1, on a five-point Likert scale. We asked the teachers' opinion about a set of specific issues: easiness of use of the models; ability to convey certain important biological concepts; and potential of interest raising and long-term engaging of students in biological studies:

Both teachers strongly agreed that the models were easy to use in the classroom. This is positive, as it demonstrates that the teachers were able to get acquainted with the model kits even with a very limited training. They also appreciated the choice of material: the rubber was deemed easy to manipulate, sturdy, and easy to be cleaned and sanitized;

Both teachers strongly agreed that our models were able to convey the association of subunits. They commented that the flexibility of rubber allowed the monomers to associate with one another, and, especially with F-actin, the different colors made the perfect joint between subunits evident. This confirms the main advantage of producing soft, flexible, and perfectly matching models to be assembled in complexes;

Similarly, both teachers strongly agreed that our models were able to convey the concept of quaternary structure. One teacher found it that students finally understood that *quaternary complex* can mean to include any number of units. This confusion may arise from the fact that *quaternary* contains the root *quater*, in Italian *quattro*, meaning *four*.

One teacher agreed and one was neutral about the ability of our models to convey the concept of shape diversity and complexity; this result can be attributed, in our opinion, to the fact that no student could actually manipulate the objects;

The teachers agreed or strongly agreed that the models conveyed the concept of size differences. This is thanks to our fabrication of proteins at a common scale of 10 millions ×. Both teachers were surprised at the difference in size among the proteins, and in particular they did not expect hemoglobin to be so small relative to the other proteins;

Teacher 1 (science high school) agreed that the models help to explain the passage from sequence to 3D structure. Teacher 2 (technical school) did not answer, as this concept was beyond her class program;

Teacher 1 agreed that the use of fabricated soft protein models was likely to raise the interest of the students in biology. She observed that students were all curious, and surprised at this *"idea simple but revolutionary"* to make them understand proteins; one student even added that *"their potential is unlimited"*. Teacher 2 disagreed: she reported that her students were in general not particularly interested in chemistry or biology. Though she confirmed that the models surely engaged their attention, she was not sure this single experience would lead to a long-term engagement;

Both teachers did not comment about the possibility that the usage of soft protein models as teaching aids would increase the chances of students considering biology for their future studies. Indeed, the limited experience of a single lesson, and with no direct manipulation of models from the students, was not deemed sufficient to form a fair

opinion. This would require a larger and long-term user study.

Besides the questionnaire, the teachers provided additional comments about strengths and weaknesses of our models, and suggestions for improvement.

Though both teachers were able to prepare their lessons with limited training material, they both remarked that additional accompanying material would have been of use for them and for the students. For the planned future user studies, we will accompany the silicone models with additional material that will help teachers and students alike, including: a brief discussion on the nature of proteins (which are highly dynamic) and of their associations in complexes (description of the generation of the complementary surfaces); a direct reference to the original studies describing the PDB models; a simplified PDB file that teachers can use to illustrate the relation between primary (sequence), secondary (skeleton), tertiary (monomer) and quaternary structure of proteins; some suggestions for decorating the protein e.g. marking the interaction surfaces, inserting ligands or post-translational modifications (Phosphate group, lipid or oligosaccharide chain, as appropriate)

The teachers also suggested a set of additional models which would be useful in the classroom: an enzyme, an antibody (IgG), the Collagen, and a membrane protein, possibly an ion channel. One of the teachers also pointed out that it could be useful to show the same protein in two different conformations. We believe this is a very useful suggestion, which is also easy to implement with our pipeline.

8. Conclusions

The availability of tangible models can bring new life to the teaching of proteins, their functionality, their mode of action and the relationships among them. With the aim of inducing a more direct experience of the proteins as objects, we have developed a method for obtaining tangible soft models of complex macromolecules, based on the atomic structures deposited in the Protein Data Bank. Our fabrication strategy, based on casting, allows a time and cost effective production of multiple copies of the desired 3D models. We fabricated a set of protein models, all at the same scale of 10 million times, which is the best scale for human perception of cellular features [31].

We tested our models in the high school setting, by providing two teachers with model kits. We received positive feedback about the capability of our models to convey important biological concepts and to engage students. The teachers also gave interesting suggestions, which we are considering for future work. Namely, we plan to include in our fabrication strategy the embedding of magnets in rubber for more intuitive docking and to stabilize assembled complexes.

The process of fabricating the models is relatively simple and can be carried out in any school equipped with any desktop 3D printer and casting material, such as silicone. Also, molds can be printed through on demand 3D printing services. The entire process (choice of protein, selection of appropriate PDB file, extraction of the relevant model, eventual alignment, handle loops control, surface processing, mold printing, support removal, silicone casting and association of monomers) can be performed by high school and undergraduate students. Nevertheless, some schools or teachers might prefer to skip the fabrication step, and purchase models as a kit. This possibility is open to further development.

Besides high schools, the use of tangible models can be of interest also for teaching at university courses, in general public education (e.g. to demonstrate binding of SARS-CoV-2 Spike protein to its cellular receptor ACE2, and the effect of new variants), and also for scientific research. Colleagues expert in structural biology may develop additional features, like surface details emphasizing properties such as hydrophobic patches, allosteric sites, or residues with electric activity.

Our aim was to develop a pipeline to improve and ease access to high-quality tangible teaching and research material, including 3D models of large and highly-complex macromolecules. In principle, any PDB entry from which a surface can be calculated could be transformed into a tangible object. Yet the choice of the molecule must be conducted with care. Some protein structures lack considerable fractions of the protein mass, others

Table 1. Teachers' answers to the questionnaire. 1: Strongly disagree; 2: Disagree; 3: Neutral; 4: Agree; 5: Strongly agree; n.a.: not answered.

	Teacher 1	Teacher 2
The models are easy to use in the classroom.	5	5
The models convey the concept of association of subunits.	5	5
The models convey the concept of quaternary structure.	5	5
The models convey the concept of shape diversity and complexity.	3	4
The models convey the concept of size difference.	4	5
The models help to explain the passage from sequence to 3D structure.	4	n.a.
The students are more interested in biology.	4	2
The students are more likely to consider biology for their future studies.	n.a.	n.a.

have been crystallized in 'forced' (e.g. bound to an antibody) or under unphysiological conditions. The constant addition of structures, derived from several techniques, will gradually alleviate this limitation.

We believe that our method can contribute to strongly enlarge the number and variety of 3D molecular models that can be fabricated, thus widening the adoption of 3D tangible models in both education and research.

Acknowledgements

References

[1] Ford, S, Minshall, T. Invited review article: Where and how 3D printing is used in teaching and education. Additive Manufacturing 2019;25:131–150. doi:10.1016/j.addma.2018.10.028.

[2] Gordeev, EG, Ananikov, VP. Widely accessible 3D printing technologies in chemistry, biochemistry and pharmaceutics: applications, materials and prospects. Russian Chemical Reviews 2020;89(12):1507. doi:10.1070/RCR4980; publisher: IOP Publishing.

[3] Stull, AT, Hegarty, M, Dixon, B, Stieff, M. Representational Translation With Concrete Models in Organic Chemistry. Cognition and Instruction 2012;30(4):404–434. doi:10.1080/07370008.2012.719956.

[4] Capel, A, Rimington, R, Lewis, M, Christie, S. 3d printing for chemical, pharmaceutical and biological applications. Nat Rev Chem 2018;2:422–436. doi:https://doi.org/10.1038/s41570-018-0058-y.

[5] Niece, BK. Custom-Printed 3D Models for Teaching Molecular Symmetry. Journal of Chemical Education 2019;96(9):2059–2062. doi:10.1021/acs.jchemed.9b00053; publisher: American Chemical Society.

[6] Griffith, KM, Cataldo, Rd, Fogarty, KH. Do-It-Yourself: 3D Models of Hydrogenic Orbitals through 3D Printing. Journal of Chemical Education 2016;93(9):1586–1590. doi:10.1021/acs.jchemed.6b00293; publisher: American Chemical Society.

[7] Moeck, P, Stone-Sundberg, J, Snyder, T, Kaminsky, W. Enlivening 300 level general education classes on nanoscience and nanotechnology with 3d printed crystallographic models. J Mater Educ 2014;36:77–96.

[8] Penny, MR, Cao, ZJ, Patel, B, Sil dos Santos, B, Asquith, CRM, Szulc, BR, et al. Three-dimensional printing of a scalable molecular model and orbital kit for organic chemistry teaching and learning. Journal of Chemical Education 2017;94(9):1265–1271. doi:10.1021/acs.jchemed.6b00953.

[9] Herman, T, Morris, J, Colton, S, Batiza, A, Patrick, M, Franzen, M, et al. Tactile teaching: Exploring protein structure/function using physical models. Biochem Mol Biol Educ 2006;34(4):247–54. doi:10.1002/bmb.2006.494034042649.

[10] Meyer, SC. 3D Printing of Protein Models in an Undergraduate Laboratory: Leucine Zippers. Journal of Chemical Education 2015;92(12):2120–2125. doi:10.1021/acs.jchemed.5b00207.

[11] Hall, S, Grant, G, Arora, D, Karaksha, A, McFarland, A, Lohning, A, et al. A pilot study assessing the value of 3D printed molecular modelling tools for pharmacy student education. Currents in Pharmacy Teaching and Learning 2017;9(4):723–728. doi:10.1016/j.cptl.2017.03.029.

[12] Coakley, MF, Hurt, DE, Weber, N, Mtingwa, M, Fincher, EC, Alekseyev, V, et al. The NIH 3D Print Exchange: A Public Resource for Bioscientific and Biomedical 3D Prints. 3D Printing and Additive Manufacturing 2014;1(3):137–140. doi:10.1089/3dp.2014.1503.

[13] Corey, RB, Pauling, L. Molecular Models of Amino Acids, Peptides, and Proteins. Review of Scientific Instruments 1953;24(8):621–627. doi:10.1063/1.1770803; publisher: American Institute of Physics.

[14] Kendrew, J, Bodo, G, Dintzis, H, Parrish, R, Wyckoff, H, Phillips, D. A three-dimensional model of the myoglobin molecule obtained by x-ray analysis. Nature 1958;181(4610):662–666. doi:10.1038/181662a0.

[15] Miao, H, Klein, T, Kouřil, D, Mindek, P, Schatz, K. Multiscale molecular visualization. Journal of Molecular Biology 2019;431(6):1049–1070. doi:ff10.1016/j.jmb.2018.09.004.

[16] Hirst, JD, Glowacki, DR, Baaden, M. Molecular simulations and visualization: introduction and overview. Faraday Discuss 2014;169:9–22. doi:10.1039/C4FD90024C.

[17] Olson, AJ. Self-assembly gets physical. Nat Nanotechnol 2015;10(8):728. URL: http://www.ncbi.nlm.nih.gov/pubmed/26243003. doi:10.1038/nnano.2015.172.

[18] Kawakami, M. A soft and transparent handleable protein model. Review of Scientific Instruments 2012;83(8). doi:10.1063/1.4739961.

[19] Berman, HM, Westbrook, J, Feng, Z, Gilliland, G, Bhat, TN, Weissig, H, et al. The Protein Data Bank. Nucleic Acids Res 2000;28(1):235–42. URL: http://www.ncbi.nlm.nih.gov/pubmed/10592235.

[20] Schrödinger, LLC, . The PyMOL molecular graphics system, version 2.4; 2015. URL: http://www.pymol.org/pymol.

[21] Connolly, M. Solvent-accessible surfaces of proteins and nucleic acids. Science 1983;221(4612):709–713. doi:10.1126/science.6879170.

[22] De Garmo, EP, Black, JT, Kohser, RA. DeGarmo's materials and processes in manufacturing. John Wiley & Sons; 2011.

[23] Wannarumon, S. Reviews of computer-aided technologies for jewelry design and casting. Naresuan University Engineering Journal 2011;6(1):45–56.

[24] Alderighi, T, Malomo, L, Giorgi, D, Pietroni, N, Bickel, B, Cignoni, P. Metamolds: Computational design of silicone molds. ACM Trans Graph 2018;37(4):136:1–136:13. doi:10.1145/3197517.3201381.

[25] Alderighi, T, Malomo, L, Giorgi, D, Bickel, B, Cignoni, P, Pietroni, N. Volume-aware design of composite molds. ACM Trans Graph 2019;38(4):110:1–110:12. doi:10.1145/3306346.3322981.

[26] Dey, TK, Fan, F, Wang, Y. An efficient computation of handle and tunnel loops via reeb graphs. ACM Transactions on Graphics (TOG) 2013;32(4):1–10.

[27] Kazhdan, M, Hoppe, H. Screened poisson surface reconstruction. ACM Trans Graph 2013;32(3). URL: https://doi.org/10.1145/2487228.2487237. doi:10.1145/2487228.2487237.

[28] Zhou, Q, Grinspun, E, Zorin, D, Jacobson, A. Mesh arrangements for solid geometry. ACM Trans Graph 2016;35(4):39:1–39:15.

[29] Emsley, P, Lohkamp, B, Scott, WG, Cowtan, K. Features and development of *Coot*. Acta Crystallographica Section D Biological Crystallography 2010;66(4):486–501. doi:10.1107/S0907444910007493.

[30] Winn, MD, Ballard, CC, Cowtan, KD, Dodson, EJ, Emsley, P, Evans, PR, et al. Overview of the *CCP* 4 suite and current developments. Acta Crystallographica Section D Biological Crystallography 2011;67(4):235–242. doi:10.1107/S0907444910045749.

[31] Zoppè, M. Towards a perceptive understanding of size in cellular biology. Nature Methods 2017;14(7):662–665. doi:10.1038/nmeth.4300.

[32] Avery, AW, Fealey, ME, Wang, F, Orlova, A, Thompson, AR, Thomas, DD, et al. Structural basis for high-affinity actin binding revealed by a β-III-spectrin SCA5 missense mutation. Nature Communications 2017;8(1):1350. doi:10.1038/s41467-017-01367-w.

[33] Paoli, M, Liddington, R, Tame, J, Wilkinson, A, Dodson, G. Crystal structure of T state haemoglobin with oxygen bound at all four haems. Journal of Molecular Biology 1996;256(4):775–792. doi:10.1006/jmbi.1996.0124.

[34] Davey, CA, Sargent, DF, Luger, K, Maeder, AW, Richmond, TJ. Solvent Mediated Interactions in the Structure of the Nucleosome Core Particle at 1.9Å Resolution. Journal of Molecular Biology 2002;319(5):1097–1113. doi:10.1016/S0022-2836(02)00386-8.

[35] Connolly, ML. Analytical molecular surface calculation. Journal of Applied Crystallography 1983;16(5):548–558. doi:10.1107/S0021889883010985.

[36] Museth, K. Vdb: High-resolution sparse volumes with dynamic topology. ACM Trans Graph 2013;32(3). doi:10.1145/2487228.2487235.

[37] Visual Computing Lab, . The VCG library. 2020. URL: http://vcg.isti.cnr.it/vcglib/.